

Enhanced Reduction of Fe(II)EDTA-NO/Fe(III)EDTA in NO_x Scrubber Solution Using a Three-Dimensional Biofilm-Electrode Reactor

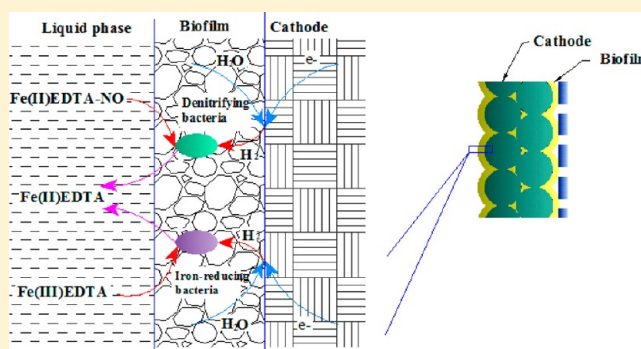
Ya Zhou,[†] Lin Gao,[‡] Yin-Feng Xia,[†] and Wei Li^{†,*}

[†]Key Laboratory of Biomass Chemical Engineering of Ministry of Education, Institute of Industrial Ecology and Environment, Zhejiang University (Yuquan Campus), Hangzhou 310027, China

[‡]Rudong Environmental Protection Bureau, Nantong 226400, China

S Supporting Information

ABSTRACT: A promising technique called chemical absorption–biological reduction (CABR) integrated approach has been developed recently for the nitrogen oxides (NO_x) removal from flue gases. The major challenge for this approach is how to enhance the rate of the biological reduction step. To tackle the challenge, a three-dimensional biofilm-electrode reactor (3D-BER) was utilized. This reactor provides not only considerable amount of sites for biofilm, but also many electron donors for bioreduction. Factors affecting the performance of 3D-BER were optimized, including material of the third electrode (graphite), glucose concentration (1000 mg·L⁻¹), and volume current density (30.53 A·m⁻³ NCC). Experimental results clearly demonstrated that this method significantly promotes the bioreduction rate of Fe(II)EDTA-NO (0.313 mmol·L⁻¹·h⁻¹) and Fe(III)EDTA (0.564 mmol·L⁻¹·h⁻¹) simultaneously. Experiments on the mechanism showed that Fe(II)EDTA serves as the primary electron donor in the reduction of Fe(II)EDTA-NO, whereas the reduction of Fe(III)EDTA took advantage of both glucose and electrolysis-generated H₂ as electron donors. High concentration of Fe(II)EDTA-NO or Fe(III)EDTA interferes the bioreduction of the other one. The proposed methodology shows a promising prospect for NO_x removal from flue gas.

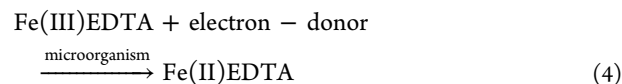
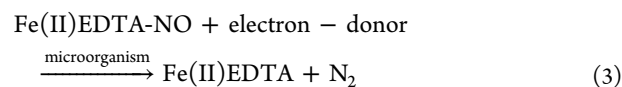
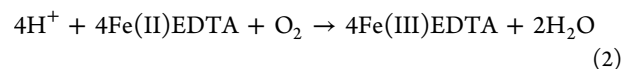
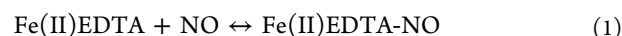


INTRODUCTION

Nitrogen oxides (NO_x), mainly nitric oxide (NO), emitted into atmosphere causes serious environmental and health problems, such as acid rain, photochemical smog, and depletion of the ozone layer. The release of nitrogen oxides during fuel combustion is considered to be one major source.^{1,2} Industrial flue gases have been treated by several approaches, such as selective catalytic reduction (SCR), selective non-catalytic reduction (SNCR), adsorption, and absorption. Although these conventional control methods could basically meet the requirements, they, respectively, suffer from the risk of second pollution and low efficiency.³

Researchers have demonstrated that bioreactors can be successfully employed for the removal of NO_x from combustion gases in a laboratory, but the high Henry's constant of NO restricts a higher efficiency of NO removal.⁴ It was confirmed through abiotic and biological removals in the biotrickling filter that NO removals in high concentration (1000 ppm or higher) were in large measure the result of abiotic removal in both gas-phase and liquid-phase reactions while bionitrification was the main process of NO removal in low concentration (less than 100 ppm).⁵ Hence a promising technique called chemical absorption-biological reduction (CABR) integrated approach has been developed recently for the NO_x removal from flue gases.^{6–8} In this approach,

Fe(II)EDTA is used to overcome the limitation of biological treatment processes by promoting the NO absorption into scrubber liquor. The nitrosyl complex can be reduced to N₂ by a group of denitrifying bacteria and Fe(III)EDTA, oxidation of Fe(II) by oxygen in the flue gas, can be reduced by dedicated iron-reducing bacteria. The CABR integrated process mainly consists of four reactions as follows:⁹



Received: June 28, 2012

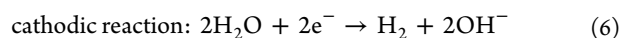
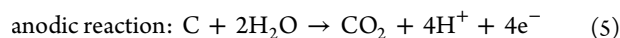
Revised: September 18, 2012

Accepted: October 31, 2012

Published: October 31, 2012

Since only Fe(II)EDTA is capable of binding NO, the NO removal efficiency in the CABR integrated process strongly depends on the concentration of Fe(II)EDTA in the scrubber liquor.^{10,11} Therefore, it is important to effectively bioreduce Fe(II)EDTA-NO and Fe(III)EDTA in this system.

In the past decades, a biofilm electrode reactor (BER) had been proposed to treat nitrate contaminated water.^{12–15} Nowadays, this method has been widely used and developed.^{16,17} In BER, immobilized microorganisms on the surface of the cathode utilize the hydrogen gas generated from electrolysis of water as electron donor.¹⁸ Electrode reactions were reported before:¹³



In this system, CO₂ yielded from the anode dissolves and turns into H₂CO₃, CO₃²⁻ and HCO₃⁻, which serve as carbon source of autotrophic microorganism as well as pH buffer. At the cathode, dissolved oxygen is first electrolyzed into OH⁻, creating an oxygen-deficient environment for denitrification, and then H₂ is generated to provide electron donors for denitrifying bacteria. Autotrophic denitrifying bacteria could use H₂ from cathode as electron donor and CO₂ from anode as inorganic carbon source. This process was widely expected to give rise to biological reaction rate.

We previously conducted a pilot study on the regeneration of ferrous chelate complexes in NO_x scrubber solution by a normal BER. Feasibility of this approach was confirmed and bioreduction of Fe(III)EDTA was found to be electrochemically accelerated.⁹ However, reduction rate of Fe(II)EDTA-NO was still low and presence of Fe(II)EDTA-NO had a strong inhibition of Fe(III)EDTA reduction. Recently, researchers in the field of BER committed themselves to optimize the electrode structure. Sakakibara and Nakayama proposed a novel multielectrode system using expanded metal as electrode for biological water treatments.¹⁴ They believed that large effective surface area of multielectrode contributes to intensifying denitrification. Zhou developed three-dimensional BERs for nitrate and organic pollutants removal, proving that the presence of activated carbon as the third bipolar electrode provided much more sites for biofilm formation and hydrogen gas yield.^{19,20} Enlightened by these results, we utilized 3D-BER to expand effective surface area of electrode, thus enhance the bioreduction of Fe(II)EDTA-NO and Fe(III)EDTA in NO_x scrubber solution. Materials of the third electrode, operating conditions and mechanism of this approach were investigated.

MATERIALS AND METHODS

Chemicals. Disodium ethylenediaminetetraacetate (Na₂EDTA, 99.95%), FeSO₄(NH₄)₂SO₄ (99.5%), FeCl₃·6H₂O (99.5%), D-glucose (99.5%, cell culture tested) were obtained from Shanghai Chemical Reagent Co.(Shanghai, China). NO (5% in N₂, v/v) and N₂ (99.999%) were obtained from Zhejiang Jingong Gas Co.(Hangzhou, China). All other chemicals were analytical grade, commercially available and used without further purification.

Fe(II)EDTA-NO and Fe(III)EDTA complexes were prepared according to our previous study.¹¹ As for the preparation of Fe(II)EDTA-NO, FeSO₄(NH₄)₂SO₄ was used to prepare

the ferrous EDTA solution instead of FeCl₂ in order to improve the oxidation tolerance. The pH was adjusted to 5.0 with 2 mmol·L⁻¹ NaOH before NO absorption.

Organism and Media. Cultures were grown in basal medium composed of the components as follows (g per liter): Glucose, 0–2.5; KH₂PO₄, 0.3; Na₂SO₃, 0.07; MgCl₂, 0.1; NaHCO₃, 5.4. Trace element solution for the bacteria growth contained the following components (g per liter): CoCl₂, 0.24; MnCl₂·4H₂O, 0.99; CuSO₄·5H₂O, 0.25; Na₂MoO₄·2H₂O, 0.22; NiCl₂·6H₂O, 0.19; H₃BO₃, 0.014; ZnCl₂, 0.1.

Microorganisms used in this study were the mixed culture of *Pseudomonas* sp. DN-2,²¹ and *Escherichia coli* FR-2,¹¹ whose GenBank accession numbers were DQ811956 and DQ411026. The two strains were deposited in the China general microbiological culture collection center and the collection numbers were CGMCC No.1753 and No.1467. After cultivation for microbial adaption, the mixed culture performed well on reducing Fe(II)EDTA-NO and Fe(III)EDTA simultaneously.

Reactor Configuration. Total volume of the cylindrical reactor was 2 L while the effective working volume was 1.2 L. Anode region and cathode region were separated by a plastic sleeve with tiny holes, in order to avoid possible short circuit. One graphite rod was installed along the central axis of the 3D-BER as the anode and four surrounded as the cathodes. Remaining space in the cathode area was filled with conductive granules, which serves not only as biofilm carrier but also as the third electrode. The function of the third electrode is to expand the cathode and thus provide another dimension. There was a diving pump to blend the solution and a DC power to supply constant current. Referring to our previous study,^{9,22} the reactor was immersed in a water bath at 323 K to simulate typical flue gas temperature (45–55 °C) after the FGD process. A schematic diagram of the continuous apparatus is shown in Figure 1.

We studied on two materials for the third electrode. One was activated carbon, which were 6–10 mm in length and 4 mm in diameter. The volume of filled granular activated carbon was about 1 L and void fraction was 37%.The other one was

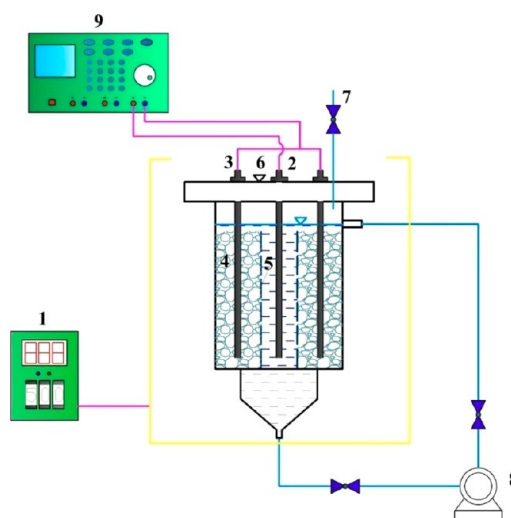


Figure 1. Configuration of the three-dimensional bioelectrode reactor. (1. water bath; 2. anode carbon rods; 3. cathode carbon rods; 4. particle electrode; 5. plastic sleeve; 6. sampling port; 7. gas exhaust pipe; 8. peristaltic pump; 9. DC power supply).

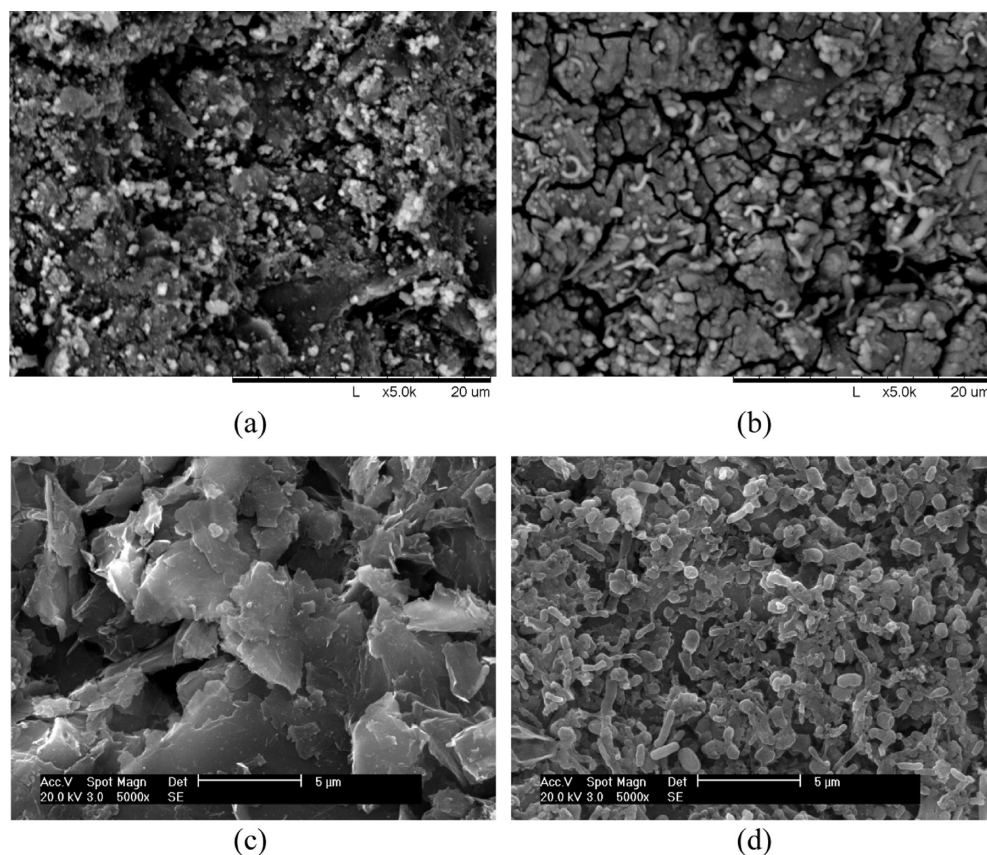


Figure 2. ESEM images of the electrode surface. (a) activated carbon, raw; (b) activated carbon, biofilm-formed; (c) graphite, roughened; (d) graphite, biofilm-formed.

graphite. Since the surface is relatively smooth, the 6 mm-diameter graphite rods were roughened by hand to provide more sites for the growth of microorganisms and then cut into 6–8 mm in length. The volume of filled graphite was 1.08 L and void fraction was 44%. All these materials were bought from Shanghai new graphite material Co., Ltd.

3D-BER Start-up. The 3D-BER was started up through batch experiments. To start a batch experiment, a solution containing 4 mmol·L⁻¹ Fe(II)EDTA-NO, 8 mmol·L⁻¹ Fe(III)-EDTA, basal medium, trace nutrients, and mixed culture, after adjusting the pH to 6.8, was fed into the reactor. 2500 mg·L⁻¹ glucose and 10 mA current was applied at the first period. When proportion of Fe(II)EDTA in total iron ion reached 85%, solution was refreshed to start a new batch experiment. If it could surpass 85% within 12 h, lower glucose concentration and stronger current intensity was applied to start a new period. After repetitions of batch reduction for months, biofilm became visible on the surface of the electrode. At the same time, performance of 3D-BER without mixed culture in the initial solution was as good as before. It could be concluded that the biofilm on the cathode had already formed and no more inoculum was needed.⁹ Formed biofilm was observed via Environmental Scan Electro-Microscope (ESEM, Philips Model XL30).

Experimental Procedure. After the biofilm was formed, 12 h batch experiments were conducted under various conditions. Components fed into the reactor were similar to the start-up process and initial total iron concentration was always 12 mmol·L⁻¹. With 4 mmol·L⁻¹ Fe(II)EDTA-NO and 8 mmol·L⁻¹ Fe(III)EDTA in the initial solution, different glucose

concentration (0–2000 mg·L⁻¹) and current intensity (0–40 mA) were applied to find out the optimum operating condition. Referring to this operating condition, performance of bioelectrochemical reduction and biological reduction of NO_x scrubber solution was investigated in the 3D-BER, while performance of electrochemical reduction was examined in an abiotic reactor. Aiming to explore the electron donors in bioreductions, four batch experiments in 3D-BER were carried out under different conditions: (i) with 1000 mg·L⁻¹ glucose and 0 mA current; (ii) with 0 mg·L⁻¹ glucose and 20 mA current; (iii) with 1000 mg·L⁻¹ glucose and 20 mA current; (iv) with 0 mg·L⁻¹ glucose and 0 mA current, and another batch experiment were carried out in abiotic reactor with 0 mg·L⁻¹ glucose and 20 mA current. Interference between the two substrates was investigated with different initial concentration of Fe(II)EDTA-NO (0–6 mmol·L⁻¹) and Fe(III)EDTA (6–12 mmol·L⁻¹).

Analytical Methods. Concentration of Fe(II)EDTA-NO was determined from a calibration curve for correlating absorbency to the concentration of Fe(II)EDTA-NO.²¹ The absorbency was directly determined by a model UV-2000 spectrophotometer (UNICO (Shanghai, China) Instruments) at 420 nm. The concentration of total ferrous ions was determined by a modified 1, 10-phenanthroline colorimetric method at 510 nm.⁷ The concentration of Fe(III)EDTA was calculated by the difference between total Fe and Fe(II). Sample solution containing microorganisms should get across micro porous membrane with 0.22 μm pore size before measured. The concentrations of H₂ and CO₂ were measured with gas chromatography (GC-7890, Agilent, USA).

All the data shown in this study were the mean values of the duplicate or triplicate experiments. Confidence level used in this article was 95% while probability of different results was determined by *t*-distribution.

RESULTS AND DISCUSSION

Comparison of the Materials of the Third Electrode.

Two reactors, with either activated carbon or graphite as the material of the third electrode, were started up and numbered, respectively, as reactor I and reactor II. In the biofilm-forming process, blockage often occurred in reactor I and led to liquid level rise. After start-up period finished, surfaces of original and biofilm-formed electrodes were observed through ESEM (Figure 2). Images showed that biomass on the surface of graphite was far more than that of activated carbon and tiny pores appearing on the surface of raw activated carbon was not found on that of biofilm-formed activated carbon.

In reactor I, total iron ion concentration in the solution (expressed as [Fe] in the following text), including Fe(II) and Fe(III), fluctuated distinctly all through the start-up process of 3D-BER. In the beginning, [Fe] showed a significant drop during the 12 h running. After a period of time, it exhibited a quite dissimilar tendency that [Fe] rose after a slight decrease. At the end of start-up process, [Fe] was relatively stable. However, even after the start-up was completed, the volatility could hardly be controlled within the error range and was nearly eight times as much as that in reactor II (Table 1). This

Table 1. Performance of Reactors with Two Different Materials As the Third Electrode

material of the third electrode	Fe(II)EDTA-NO reduction efficiency	Fe(III)EDTA reduction efficiency	Fe(II)EDTA formation efficiency	volatility of total iron ion concentration
activated carbon	92–94.2%	34–66.5%	68–80.9%	16.1%
graphite	90–93.1%	58–67.4%	76–85.3%	2.17%

could be due to the strong adsorption of activated carbon, which also caused the blockage in reactor I as mentioned above. The fluctuation of [Fe] severely influenced the stable performance of the reactor, so that it must be counted when we select the material of the third electrode.

Ranges of chelate complexes reduction efficiencies listed in Table 1 were obtained from multiple 12 h test cycles, where the initial concentration of both Fe(II)EDTA-NO and Fe(III)EDTA was 6 mmol·L⁻¹. The two reactors gave almost the same reduction efficiency of Fe(II)EDTA-NO, which was higher than 90%. As to the reduction of Fe(III)EDTA, reactor I exhibited a lower efficiency and a greater fluctuation. Overall, reactor II presented a better formation efficiency of Fe(II)EDTA.

Activated carbon was reported as suitable material of the third electrode due to its considerable surface area, good electrical conductivity, high mechanical strength and low cost. Nevertheless, owing to its strong adsorption properties, tiny pores on the surface would be covered by the deposition of pollutants and reaction products. It leads to a series of problems, such as blockage, fewer adherences of micro-organism, lower reduction efficiency, and less stability. On the other hand, graphite has equally good electrical conductivity and no these problems. Based on the above considerations,

graphite was selected as the material of the third electrode so that reactor II was utilized in the following study.

Operating Conditions Affecting 3D-BER Performance.

Glucose has been used as carbon source due to its high reduction rate for Fe(II)EDTA-NO in our previous study. Certain concentration (0–2000 mg·L⁻¹) of glucose was added into the reactor to investigate the effects of glucose concentration on the reduction. Correlation between reduction rate of Fe(II)EDTA-NO and glucose concentration was unremarkable. On the other hand, glucose concentration had a relatively obvious influence on the reduction of Fe(III)EDTA. It could be preliminarily concluded from the results that glucose is not the primary electron donor in the bioreduction of Fe(II)EDTA-NO but probably one of the main electron donors in the reduction of Fe(III)EDTA. Table 2 provides the details

Table 2. Fe(II)EDTA Formation Rate in Different Glucose Concentration and Volume Current Density

glucose concentration (mg·L ⁻¹)	volume current density (A·m ⁻³ NCC ^a)	Fe(II)EDTA formation rate (mmol·L ⁻¹ ·h ⁻¹)	current efficiency (%)
0	30.53	0.568	N/A
100	30.53	0.603	N/A
200	30.53	0.650	N/A
500	30.53	0.850	N/A
1000	30.53	0.810	N/A
2000	30.53	0.805	N/A
0	0	0.123	N/A
0	15.27	0.166	53.5
0	22.90	0.315	67.6
0	30.53	0.519	83.4
0	45.80	0.625	67.0
0	61.07	0.798	64.1

^aNCC: Net Cathodic Compartment.

of Fe(II)EDTA average formation rate, which reached the highest of 0.850 mmol·L⁻¹·h⁻¹ when glucose concentration was 500 mg·L⁻¹. As a relatively higher level of microorganism amount and activity could be better for long-time sustainable operation, we selected 1000 mg·L⁻¹ as the concentration of glucose.

Since impact of volume current density on the reduction would be more evident without external carbon source, glucose was no longer added when volume current density was studied. Results showed that reduction of Fe(III)EDTA rather than Fe(II)EDTA-NO was directly bound up with electric current in the range of 0–40 mA. Reduction efficiency and rate of Fe(III)EDTA rose along with the current increase and there was no inhibition of denitrification by current increase, which was also reported in former research.^{23,24} As to the Fe(II)EDTA formation rate, Table 2 shows it continuously increased from 0.123 mmol·L⁻¹·h⁻¹ to 0.798 mmol·L⁻¹·h⁻¹. However, it could be inferred that further increase of current would have negative effect on the reduction through destructing the enzyme activity in cells and generating too much hydrogen to immobilize the biofilm. Current efficiency confirmed this tendency. It achieved the maximum of 83.4% when 20 mA electricity (volume current density = 30.53 A·m⁻³ NCC) was applied and presented a decline with further current increase.

With glucose concentration of 1000 mg·L⁻¹ and electric current of 20 mA, the average formation rate of Fe(II)EDTA reached 83.7%. Average reduction rate of Fe(II)EDTA-NO and

Fe(III)EDTA was $0.313 \text{ mmol}\cdot\text{L}^{-1}\cdot\text{h}^{-1}$ and $0.564 \text{ mmol}\cdot\text{L}^{-1}\cdot\text{h}^{-1}$, much higher than $0.04 \text{ mmol}\cdot\text{L}^{-1}\cdot\text{h}^{-1}$ and $0.201 \text{ mmol}\cdot\text{L}^{-1}\cdot\text{h}^{-1}$ in a 2D-BER in previous study.²⁵ With such an excellent performance, these operating conditions were applied in the following experiments.

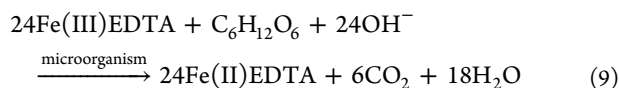
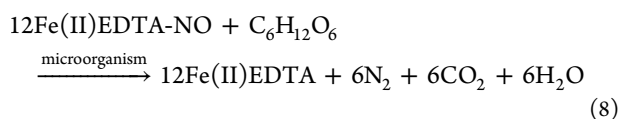
Fe(II)EDTA-NO Reduction, Fe(III)EDTA Reduction, and Fe(II)EDTA Formation by Three Different Methods. Results of Fe(II)EDTA formation via Fe(II)EDTA-NO and Fe(III)EDTA reduction by three different methods (biological, electrochemical or bioelectrochemical) are shown in Figure 3.

In the electrochemical system, Fe(II)EDTA-NO could be reduced by 50.7% after 12 h (Figure 3-a). The reduction by biological and bioelectrochemical system reached 77.7% and 79.1%, respectively, and was almost accomplished in 6 h. The advantage of bioelectrode system was not obvious.

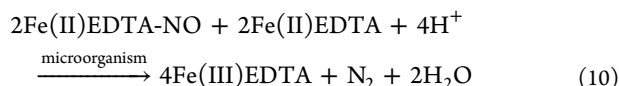
The addition of electrochemical approach considerably improved the reduction of Fe(III)EDTA. Since the reactor was sealed not so perfectly, there was a little bit oxygen. Reduction of Fe(III)EDTA by 20 mA electricity was too subtle to counteract the oxidation and its concentration showed a continuous slight rise (Figure 3-b), while that in biological system experienced a decline of 44% after the rise in the first 1.5 h. Only in the bioelectrode system did Fe(III)EDTA concentration show a persistent drop of 77%, much higher than sum of the other two systems. As to the reaction rate, concentration of Fe(III)EDTA decreased obviously slower in the first 3 h than the next 6 h, and stabilized in the last 3 h.

Figure 3-c shows the formation of Fe(II)EDTA. After 12 h, Fe(II)EDTA proportion in total iron ion concentration reached 2.5%, 58.1%, and 83.2%, respectively, in electrochemical, biological, and bioelectrode system. The ultimate proportion in sole biological system could also reach 83.5%, but much more time was needed. All these results doubtlessly confirmed that the 3D-BER we proposed acts feasibly and efficiently on the reduction of the chelate complexes.

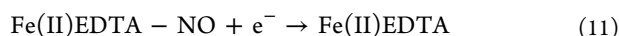
Electron Donors in the Reduction of Fe(II)EDTA-NO and Fe(III)EDTA. Regeneration of Fe(II)EDTA from the Fe(II)EDTA-NO and Fe(III)EDTA with glucose as electron donor proceeds according to²⁶



It was reported that the absorbent itself, Fe(II)EDTA, can also serve as electron donor for the biological reduction of Fe(II)EDTA-NO to N_2 according to²⁷



With electricity applied, direct electrochemical reduction possible to take place at the cathode are shown as follows:^{27,28}



Moreover, hydrogen generated through reaction 6 could also be used as electron donor in the reductions.

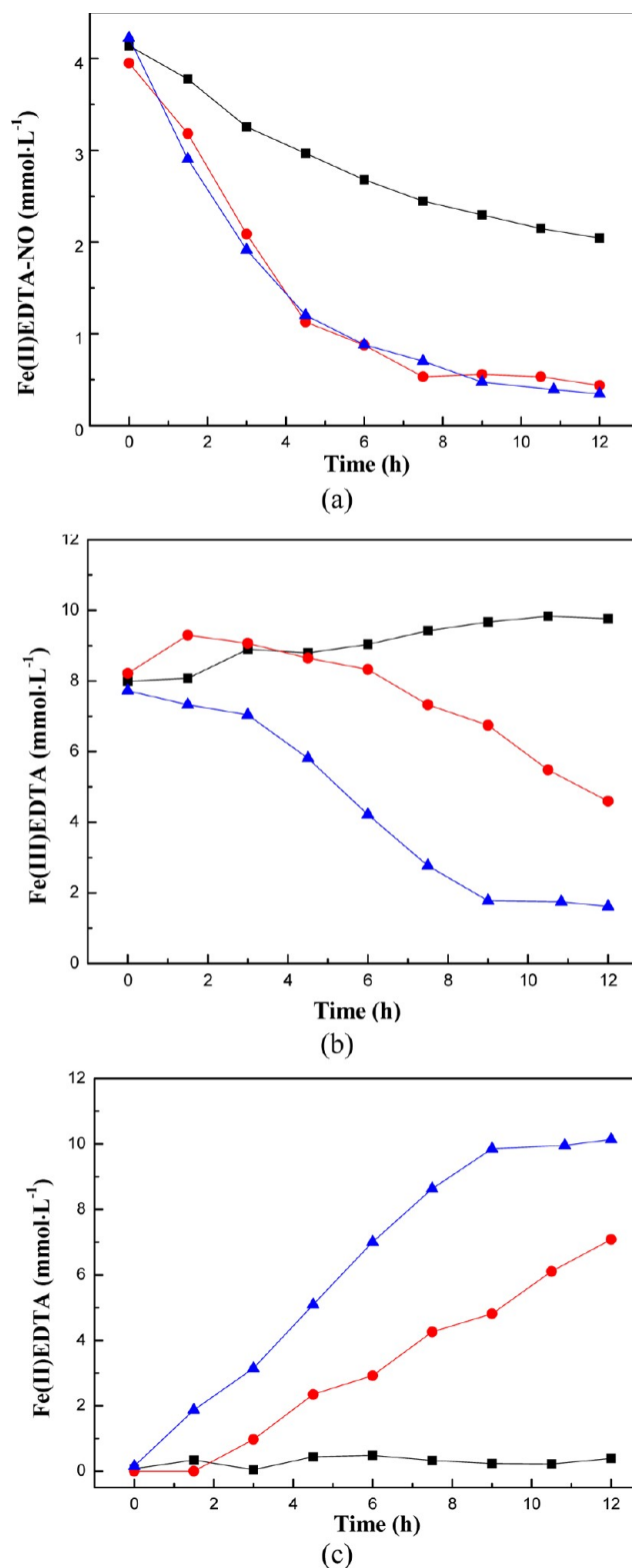


Figure 3. Fe(II)EDTA-NO reduction (a), Fe(III)EDTA reduction (b), Fe(II)EDTA formation (c) in three different systems. (black square) electrochemical; (red circle) biological; (blue triangle) bioelectrochemical. ($T = 323 \text{ K}$, $[\text{Fe(III)EDTA}]_0 = \sim 8 \text{ mmol}\cdot\text{L}^{-1}$, $[\text{Fe(II)EDTA-NO}]_0 = \sim 4 \text{ mmol}\cdot\text{L}^{-1}$, $\text{pH } 6.8$).

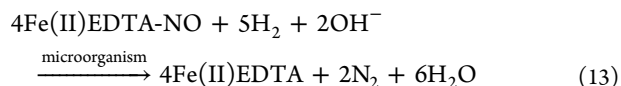
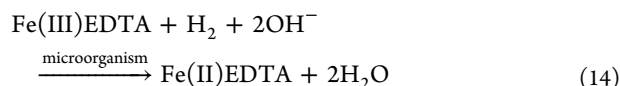


Table 3. Batch Experiments Conditions for the Investigation of Electron Donors ((+): With Reaction; (-): Without Reaction)

batch	reduction of Fe(II)EDTA-NO				reduction of Fe(III)EDTA		
	reaction 8	reaction 10	reaction 11	reaction 13	reaction 9	reaction 12	reaction 14
1	+	+	-	-	+	-	-
2	-	+	+	+	-	+	+
3	+	+	+	+	+	+	+
4	-	+	-	-	-	-	-
5	-	-	+	-	-	+	-



Glucose, electricity, and microorganisms were, respectively, controlled in five batches of experiments in order to find out the dominant electron donors in the reduction of Fe(II)EDTA-NO and Fe(III)EDTA. Condition details are provided in Table 3 and results are given in Figure 4.

Figure 4-a gives the results of Fe(II)EDTA-NO reduction. Reduction efficiency of Fe(II)EDTA-NO reached the lowest with electrochemical reduction only (batch 5). Electrochemical reduction was excluded from the main Fe(II)EDTA-NO-reducing reaction. Reduction efficiency presented hardly difference between experiments with and without electricity in 3D-BER (batch 1 and batch 3). Electrolysis-generated H₂ was also excluded. The same situation happened to glucose (batch 2 and batch 3). On the basis of the above, dominant electron donor in the reduction of Fe(II)EDTA-NO should be Fe(II)EDTA. High efficiency with Fe(II)EDTA as the only electron donor (batch 4) confirmed the speculation. It has been reported that when both electricity and an external source of organic matter were supplied to the reactor, the denitrification rate was enhanced due to simultaneous utilization of hydrogen gas derived from electrolysis and the added organic matter.^{29,30} However, our results presented that denitrification bacteria in the reactor are mostly chemoautotrophic. Van der Mass reported similar results.³¹

Results of Fe(III)EDTA reduction are given in Figure 4-b. Twenty mA electricity in abiotic reactor could hardly cancel out the accumulation of Fe(III)EDTA caused by oxidation (batch 5), but better than no feasible way in 3D-BER (batch 4). It could be inferred that electrochemical reduction contributes little to the reduction of Fe(III)EDTA. Reduction efficiency of Fe(III)EDTA with both electricity and glucose was almost the sum of that with either electricity or glucose (batch 1, 2, and 3), which could lead to the conclusion that the reduction of Fe(III)EDTA uses both electrolysis-generated H₂ and glucose as electron donors. The result also indicates that the iron-reducing bacteria consist of both autotrophic and heterotrophic microorganisms.

In sole electrochemical approach, Fe(II)EDTA was transformed from Fe(II)EDTA-NO and Fe(III)EDTA with reaction 11 and 12. The Coulombic efficiency in the bioelectrochemical system is defined as the percentage of supplied electrons that were converted to P product:³²

$$e = \frac{([P]_{t_2} - [P]_{t_1})VnF}{\int_{t_1}^{t_2} Idt} \times 100\%$$

Where e is the Coulombic efficiency, t is time (s), $[P]_t$ is product concentration at time = t (mol·L⁻¹), V is volume (L), n is number of electrons involved in the reduction, F is the

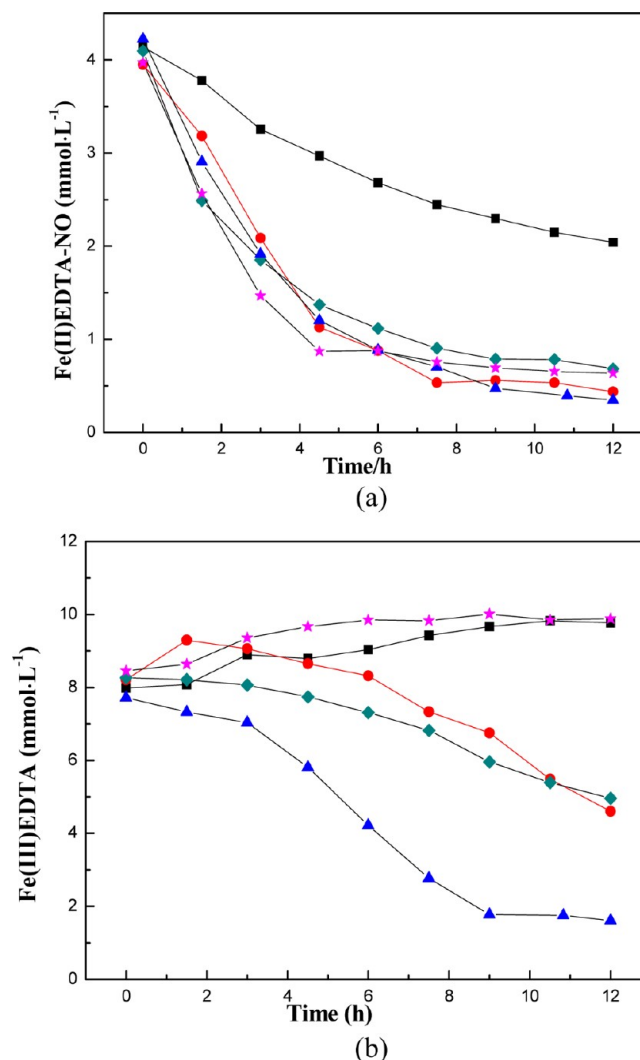


Figure 4. Reduction of Fe(II)EDTA-NO (a) and Fe(III)EDTA (b) under different reducing pathway. (red circle) Batch 1: 1000 mg·L⁻¹ Glucose, $I = 0$ mA, 3D-BER; (open blue square) Batch 2: 0 mg·L⁻¹ Glucose, $I = 20$ mA, 3D-BER; (blue triangle) Batch 3: 1000 mg·L⁻¹ Glucose, $I = 20$ mA, 3D-BER; (open red square) Batch 4: 0 mg·L⁻¹ Glucose, $I = 0$ mA, 3D-BER; (black square) Batch 5: 0 mg·L⁻¹ Glucose, $I = 20$ mA, abiotic reactor. ($T = 323$ K, $[\text{Fe(III)EDTA}]_0 = 8$ mmol·L⁻¹, $[\text{Fe(II)EDTA-NO}]_0 = \sim 4$ mmol·L⁻¹, pH 6.8).

Faraday constant (C·mol⁻¹), and I is current (A). The electron equivalents that might derive from the inoculum were disregarded in the calculation. According to the data in Figure 3-c, Fe(II)EDTA was produced with a conversion efficiency of 4.22% within 12 h. Assuming that the remaining 95.78% electrons were utilized on the electrode through reaction 6, we could calculate the theoretical amount of electrolysis-generated H₂ in the 12 h as 4.29 mmol. However, the amount of H₂ in the

3D-BER after 12 h of normal operating was detected as 1.63 mmol, indicating that 2.66 mmol H_2 was used as electron donors in the bioreductions. Meanwhile, H_2 was not found in 3D-BER after 6 h of normal operating, indicating that all the electrolysis-generated H_2 until then had been used. The result was in accordance with Figure 3, which shows that the bioreductions were almost finished after 8 h.

Theoretical amount of CO_2 produced on the anode could be calculated as 2.15 mmol, whereas the amount of CO_2 in the 3D-BER after 6 h of normal operating was monitored as 8.41 mmol. The increase was largely due to microbial metabolism. At the same time, we also examined HCO_3^- and volatile fatty acid (VFA) in the liquid via titrimetry. HCO_3^- after 6 h was 6.40 mmol less than that in initial solution and VFA after 6 h was 9.30 mmol more than that in initial solution. We could see that glucose was transformed to VFA through microbial metabolism, which may increase the acidity. However, HCO_3^- serve as good pH buffer, thus the pH change in 6 h was quite subtle.

To sum up, Fe(II)EDTA-NO was reduced to N_2 by denitrifying bacteria with Fe(II)EDTA as the dominant electron donor (Reaction 10) and Fe(III)EDTA was reduced to Fe(II)EDTA by iron-reducing bacteria with both electrolysis-generated H_2 and glucose as the dominant electron donors (Reaction 9 and 14). Therefore, the application of electricity directly enhanced the reduction of Fe(III)EDTA through providing electrolysis-generated H_2 to serve as electron donor and thus indirectly enhanced the reduction of Fe(II)EDTA-NO.

Interferences between the Substrates in the 3D-BER.

Various ratio of Fe(II)EDTA-NO and Fe(III)EDTA was added into 3D-BER and Fe(II)EDTA-NO could all be reduced efficiently (Figure 5-a). As concentration of Fe(III)EDTA increases, reduction rate of Fe(II)EDTA-NO decreases accordingly as listed in Table 3. The effects of chelate complexes proportion on the reduction of Fe(III)EDTA are shown in Figure 5-b. When the concentration of Fe(II)EDTA-NO was 6 mmol·L⁻¹, the reduction rate of Fe(III)EDTA was approximately zero in the first 3 h and took a head-turning rise when Fe(II)EDTA-NO decreased to 2.6 mmol·L⁻¹. In contrast, Fe(III)EDTA was reduced fast from the very beginning when there was no Fe(II)EDTA-NO in the solution.

Results showed that Fe(II)EDTA-NO and Fe(III)EDTA had inhibition to each other's microbial reduction. The phenomenon fit close to previous studies,¹¹ where the fact was confirmed that the growth of microbial strain FR-2 almost completely bogged down when the concentration of Fe(II)EDTA-NO reached 3.7 mmol·L⁻¹. However, in that process, the average reduction rate of Fe(III)EDTA in the first 6 h was 1.23 mmol·L⁻¹·h⁻¹ when Fe(II)EDTA-NO was absent, whereas it was 1.61 mmol·L⁻¹·h⁻¹ in 3D-BER. When initial solution consisted of 2 mmol·L⁻¹ Fe(II)EDTA-NO and 10 mmol·L⁻¹ Fe(III)EDTA, the average reduction rate of Fe(III)EDTA was 1.15 mmol·L⁻¹·h⁻¹ in 3D-BER. While in normal BER, it was 0.40 mmol·L⁻¹·h⁻¹, and even if there was no Fe(II)EDTA-NO and current intensity was 30 mA, the reduction rate of Fe(III)EDTA could only reach 0.47 mmol·L⁻¹·h⁻¹.²⁵ For the reduction efficiency of Fe(II)EDTA-NO, when initial solution contained 8 mmol·L⁻¹ Fe(III)EDTA and 4 mmol·L⁻¹ Fe(II)EDTA-NO, it was 79.1% within the first 6 h. While in sole biological reduction, it was only 50.6%.²¹ We could conclude from these results that, although interferences still exist, 3D-

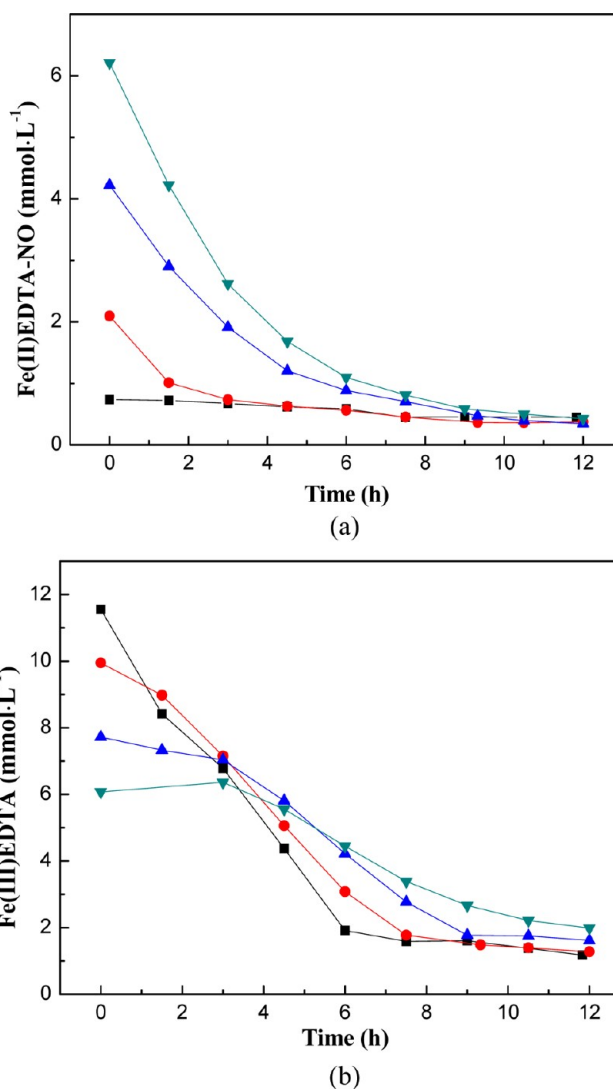


Figure 5. Reduction of Fe(II)EDTA-NO reduction (a) and Fe(III)EDTA reduction (b) in different chelate complexes proportion. (black square) $[Fe(II)EDTA-NO]_0 = 0 \text{ mmol}\cdot\text{L}^{-1}$, $[Fe(III)EDTA]_0 = 12 \text{ mmol}\cdot\text{L}^{-1}$; (red circle) $[Fe(II)EDTA-NO]_0 = 2 \text{ mmol}\cdot\text{L}^{-1}$, $[Fe(III)EDTA]_0 = 10 \text{ mmol}\cdot\text{L}^{-1}$; (blue triangle) $[Fe(II)EDTA-NO]_0 = 4 \text{ mmol}\cdot\text{L}^{-1}$, $[Fe(III)EDTA]_0 = 8 \text{ mmol}\cdot\text{L}^{-1}$; (green triangle) $[Fe(II)EDTA-NO]_0 = 6 \text{ mmol}\cdot\text{L}^{-1}$, $[Fe(III)EDTA]_0 = 6 \text{ mmol}\cdot\text{L}^{-1}$. ($T = 323 \text{ K}$, $I = 20 \text{ mA}$, $pH 6.8$).

BER presents much higher reduction rate and processing load than sole bioreduction and normal BER.

■ ASSOCIATED CONTENT

Supporting Information

Total iron ion concentration within 12 h during the start-up of Reactor I; ESEM image of the graphite surface (raw and roughened). This material is available free of charge via the Internet at <http://pubs.acs.org>.

■ AUTHOR INFORMATION

Corresponding Author

*Fax: 86-571-87952771; e-mail: w_li@zju.edu.cn.

Notes

The authors declare no competing financial interest.

ACKNOWLEDGMENTS

The work was sponsored by the National High Technology Research and Development Program of China (No. 2006AA06Z345) and the National Natural Science Foundation of China (No. 21276233).

REFERENCES

- (1) Thomas, K. M. The release of nitrogen oxides during char combustion. *Fuel* **1997**, *76* (6), 457–473.
- (2) Sun, Q. H.; Lu, Y. Q.; Fu, L. X.; Tian, H. Z.; Hao, J. M. Adjustment on NO_x emission factors and calculation of NO_x emissions in China in the year 2000. *Tech. Equip. Environ. Pollut. Control* **2004**, *5* (2), 90–94.
- (3) Radojevic, M. Reduction of nitrogen oxides in flue gases. *Environ. Pollut.* **1998**, *102*, 685–689.
- (4) Niu, H.; Leung, D. Y. C. A review on the removal of nitrogen oxides from polluted flow by bioreactors. *Environ. Rev.* **2010**, *18*, 175–189.
- (5) Chen, J. M.; Ma, J. F. Abiotic and biological mechanisms of nitric oxide removal from waste air in biotrickling filters. *J. Air Waste Manage. Assoc.* **2006**, *56*, 32–36.
- (6) Buisman, C. J. N.; Dijkman, H.; Verbraak, P. L.; Den Hartog, A. J. Process for purifying flue gas containing nitrogen oxides. *Biostar. Dev.* **1999**, Gaasterlân-Sleat US Patent US891408.
- (7) Li, W.; Wu, C. Z.; Shi, Y. Metal chelate absorption coupled with microbial reduction for the removal of NO_x from flue gas. *J. Chem. Technol. Biotechnol.* **2006**, *81*, 306–311.
- (8) Zhang, S. H.; Mi, X. H.; Cai, L. L.; Jiang, J. L.; Li, W. Evaluation of complexed NO reduction mechanism in a chemical absorption-biological reduction integrated NO_x removal system. *Appl. Microbiol. Biotechnol.* **2008**, *79*, 537–544.
- (9) Gao, L.; Mi, X. H.; Zhou, Y.; Li, W. A pilot study on the regeneration of ferrous chelate complex in NO_x scrubber solution by a biofilm electrode reactor. *Bioresour. Technol.* **2011**, *102*, 2605–2609.
- (10) Kumaraswamy, R.; Sjollem, K.; Kuenen, J. G.; van Loosdrecht, M. C. M.; Muyzer, G. Nitrate-dependent [Fe(II)EDTA]²⁻ oxidation by *Paracoccus ferrooxidans* sp. nov., isolated from a denitrifying bioreactor. *Syst. Appl. Microbiol.* **2006**, *29*, 276–286.
- (11) Li, W.; Wu, C. Z.; Zhang, S. H.; Shao, K.; Shi, Y. Evaluation of microbial reduction of Fe(III)EDTA in a chemical absorption-biological reduction integrated NO_x removal system. *Environ. Sci. Technol.* **2007**, *41*, 639–644.
- (12) Sakakibara, Y.; Kuroda, M. Electric prompting and control of denitrification. *Biotechnol. Bioeng.* **1993**, *42*, 535–537.
- (13) Sakakibara, Y.; Araki, K.; Watanabe, T.; Kuroda, M. The denitrification and neutralization performance of an electrochemically activated biofilm reactor used to treat nitrate-contaminated groundwater. *Water Sci. Technol.* **1997**, *36* (1), 61–68.
- (14) Sakakibara, Y.; Nakayama, T. A novel multi-electrode system for electrolytic and biological water treatments: Electric charge transfer and application to denitrification. *Water Res.* **2001**, *35* (3), 768–778.
- (15) Prosnansky, M.; Sakakibara, Y.; Kuroda, M. High-rate denitrification and SS rejection by biofilm-electrode reactor (BER) combined with microfiltration. *Water Res.* **2002**, *36*, 4801–4810.
- (16) Ghafari, S.; Hasan, M.; Aroua, M. K. Bio-electrochemical removal of nitrate from water and wastewater—A review. *Bioresour. Technol.* **2008**, *99*, 3965–3974.
- (17) Zhao, Y. X.; Zhang, B. G.; Feng, C. P.; Huang, F. Y.; Zhang, P.; Zhang, Z. Y.; Yang, Y. N.; Sugiura, N. Behavior of autotrophic denitrification and heterotrophic denitrification in an intensified biofilm-electrode reactor for nitrate-contaminated drinking water treatment. *Bioresour. Technol.* **2012**, *107*, 159–165.
- (18) Park, H. I.; Kim, D. K.; Choi, Y.; Pak, D. Nitrate reduction using an electrode as direct electron donor in a biofilm-electrode reactor. *Proc. Biochem.* **2005**, *40*, 3383–3388.
- (19) Zhou, M. H.; Fu, W. J.; Gu, H. Y.; et al. Nitrate removal from groundwater by a novel three-dimensional electrode-bio-film reactor. *Electrochim. Acta* **2007**, *52* (19), 6052–6059.
- (20) Zhou, M. H.; Wang, W.; Chi, M. L. Enhancement on the simultaneous removal of nitrate and organic pollutants from groundwater by a three-dimensional bio-electrochemical reactor. *Bioresour. Technol.* **2009**, *100*, 4662–4668.
- (21) Zhang, S. H.; Li, W.; Wu, C. Z.; Chen, H.; Shi, Y. Reduction of Fe(II)EDTA-NO by a newly isolated *Pseudomonas* sp. strain DN-2 in NO_x scrubber solution. *Appl. Microbiol. Biotechnol.* **2007**, *76*, 1181–1187.
- (22) Zhang, S. H.; Cai, L. L.; Mi, X. H.; Jiang, J. L.; Li, W. NO_x removal from simulated flue gas by chemical absorption-biological reduction integrated approach in a biofilter. *Environ. Sci. Technol.* **2008**, *42* (10), 3814–3820.
- (23) Sakakibara, Y.; Flora, J. R. V.; Suidan, M. T. Modeling of electrochemically-activated denitrifying biofilm. *Water Res.* **1994**, *28* (5), 1077–1086.
- (24) Flora, J. R. V.; Suidan, M. T.; Masao, K. Numerical modeling of a biofilm-electrode reactor used for enhanced denitrification. *Water Sci. Technol.* **1994**, *29* (10-11), 517–524.
- (25) Mi, X. H. A new approach for Fe(II)EDTA-NO and Fe(III)EDTA reduction in NO_x scrubber solution using bio-electro reactor. Master's thesis; Zhejiang University: Hangzhou, CN, 2010 (in Chinese).
- (26) Mi, X. H.; Gao, L.; Zhang, S. H.; Cai, L. L.; Li, W. A new approach for Fe(III)EDTA reduction in NO_x scrubber solution using bio-electro reactor. *Bioresour. Technol.* **2009**, *100*, 2940–2944.
- (27) Maas, Van der P.; Sandt, Van de T.; Klapwijk, B.; Lens, P. Biological reduction of nitric oxide in aqueous Fe(II)EDTA solutions. *Biotechnol. Prog.* **2003**, *19*, 1323–1328.
- (28) Kleifges, K. H.; Juzeliūnas, E.; Jüttner, K. Electrochemical study of direct and indirect NO reduction with complexing agents and redox mediator. *Electrochim. Acta* **1997**, *42* (9), 2947–2953.
- (29) Kuroda, M.; Watanabe, T.; Umedu, Y. High-rate denitrification of nitrate-polluted water by a bio-electro reactor process. *J. Jpn. Soc. Water Environ.* **1994**, *17*(10), 623–631 (in Japanese).
- (30) Kuroda, M.; Watanabe, T.; Umedu, Y. Simultaneous oxidation and reduction treatments of polluted water by a bio-electro reactor. *Water Sci. Technol.* **1996**, *34* (9), 101–108.
- (31) Maas, Van der P.; Harmsen, L.; Weelink, S.; Klapwijk, B.; Lens, P. Denitrification in aqueous FeEDTA Solutions. *Chem. Technol. Biotechnol.* **2004**, *79*, 835–841.
- (32) Kirsten, J. J. Bioelectrochemical ethanol production through mediated acetate reduction by mixed cultures. *Environ. Sci. Technol.* **2010**, *44*, 513–517.